JOURNAL OF GEOPHYSICAL RESEARCH, VOL. 99, NO. A12, PAGES 23,329–23,338, DECEMBER 1, 1994

Heating of the nighttime *D* region by very low frequency transmitters

Juan V. Rodriguez,[1] Umran S. Inan, and Timothy F. Bell
Space, Telecommunications and Radioscience Laboratory, Stanford University, Stanford, California

Abstract. VLF signals propagating in the Earth-ionosphere waveguide are used to probe the heated nighttime *D* region over three U.S. Navy very low frequency (VLF, 3–30 kHz) transmitters. Ionospheric cooling and heating are observed when a transmitter turns off and on in the course of normal operations. Heating by the 24.0-kHz NAA transmitter in Cutler, Maine, (1000 kW radiated power) was observed by this method in 41 of 52 off/on episodes during December 1992, increasing the amplitude and retarding the phase of the 21.4-kHz NSS probe wave propagating from Annapolis, Maryland, to Gander, Newfoundland, by as much as 0.84 dB and 5.3°, respectively. In 6 of these 41 episodes, the amplitude of the 28.5-kHz NAU probe wave propagating from Puerto Rico to Gander was also perturbed by as much as 0.29 dB. The latter observations were unexpected due to the > 770 km distance between NAA and the NAU-Gander great circle path. Heating by the NSS (21.4 kHz, 265 kW) and NLK (24.8 kHz, 850 kW) transmitters was observed serendipitously in data from earlier measurements of the amplitudes of VLF signals propagating in the Earth-ionosphere waveguide. A three-dimensional model of wave absorption and electron heating in a magnetized, weakly ionized plasma is used to calculate the extent and shape of the collision frequency (i.e., electron temperature) enhancement above a VLF transmitter. The enhancements are annular, with a geomagnetic north-south asymmetry and a radius at the outer half-maximum of the collision frequency enhancement of about 150 km. Heating by the NAA transmitter is predicted to increase the nighttime *D* region electron temperature by as much as a factor of 3. The calculated changes in the *D* region conductivity are used in a three-dimensional model of propagation in the Earth-ionosphere waveguide to predict the effect of the heated patch on a subionospheric VLF probe wave. The range of predicted scattered field amplitudes is in general consistent with the observed signal perturbations. Discrepancies in the predictions are attributed to lack of knowledge of the *D* region electron density profile along the probe wave great circle paths.

Introduction

The first experimental evidence for heating of the nighttime *D* region by very low frequency (VLF) transmitters [*Inan*, 1990a], discussed earlier from a theoretical point of view by *Galejs* [1972], involved heating by the 28.5-kHz NAU transmitter in Aguadilla, Puerto Rico. Calculations using three-dimensional models of heating and propagation in the Earth-ionosphere waveguide under different *D* region electron density profiles were consistent with observations [*Inan et al.*, 1992]. We present new experimental evidence demonstrating that powerful VLF transmitters can substantially heat the nighttime *D* region overhead on a regular basis and produce easily detectable changes in other VLF signals propagating in the Earth-ionosphere waveguide.

Experimental Results

In recent years, Stanford University has conducted VLF remote sensing experiments at multiple sites across the continental United States and Canada [e.g., *Inan et al.*, 1990] and Antarctica [e.g., *Burgess and Inan*, 1993]. These observations rely on narrowband (±150 or ±250 Hz), high-time-resolution (10, 20, or 50 ms) recordings of the amplitudes and phases of VLF transmitter signals ("probe waves") propagating in the Earth-ionosphere waveguide (Table 1). The data sets examined consist of continuous recordings on digital magnetic tape made typically at night for up to 12 hours and summary charts printed daily and archived for quick look purposes.

The original purpose of such observations was to study the spatial distribution and occurrence characteristics of localized and transient increases in the nighttime *D* region electron density that occur in association with atmospheric lightning discharges [e.g., *Inan et al.*, 1990]. In 1989, the first experimental evidence for VLF transmitter heating [*Inan*, 1990a] was discovered in the course of a controlled VLF wave-injection experiment designed to induce the precipitation of energetic radiation belt electrons using the NAU transmitter in Aguadilla, Puerto Rico, operating at 28.5 kHz and radiating a total power of 100 kW. Ionospheric heating by NAU was detected using subionospheric VLF probe waves monitored at Palmer Station, Antarctica, for the original purpose of observing transmitter-induced electron precipitation.

This serendipitous discovery led to the suggestion [*Inan*,

[1] Now at Phillips Laboratory, Geophysics Directorate, Hanscom Air Force Base, Massachusetts.

Paper number 94JA02001.
0148-0227/94/94JA-02001$05.00

Table 1. VLF and LF Transmitter Sources of Subionospheric Probe Waves

Call Letters	Frequency, kHz	Latitude, N	Longitude, W	Site Name
NSS	21.4	38°59′	76°27′	Annapolis, Maryland
NPM	23.4	21°25′	158°09′	Lualualei, Oahu, Hawaii
NAA	24.0	44°39′	67°17′	Cutler, Maine
NLK	24.8	48°12′	121°55′	Jim Creek, Washington
NAU	28.5	18°25′	67°09′	Aguadilla, Puerto Rico
—	48.5	41°30′	97°36′	Silver Creek, Nebraska

1990b] of heating experiments with the more powerful (1000 kW) NAA transmitter in Cutler, Maine (Figure 1). In this experiment, ionospheric heating by the 24.0-kHz NAA transmitter is measured using the 21.4-kHz NSS signal propagating from Annapolis, Maryland, to Gander, Newfoundland (NSS-GA), as the primary probe wave (Figure 1). Although plans to operate NAA in specially designed modulation patterns (in collaboration with and by courtesy of the U.S. Navy) have not yet been realized, cross-modulation of the NSS-GA probe wave amplitude and phase was observed at times when NAA turned off in the course of normal operations for durations of < 1 s to several hours (referred to here as off/on episodes). By analogy with the NAU heating results, it was hypothesized that these cross-modulation events were signatures of ionospheric heating by NAA.

Similar cross-modulation suggestive of ionospheric heating was found subsequently in single off/on episodes in data (amplitude only) from two other suitable VLF heater-probe wave configurations: the NPM-Saskatoon probe wave detecting heating by NLK (Figure 4) and the NAA-Huntsville probe wave detecting heating by NSS (Figure 6). In each case, one month of summary plots of narrowband probe wave amplitudes (and phases, in the case of Gander), selected based on data availability, was examined for heater off/on episodes.

The NAA Transmitter as an Ionospheric Heater

At Gander, two 1.7 m × 1.7 m vertical loops (made of 11 turns of wire) were erected so that the NAA signal was nulled on antenna A and received nearly at full strength on antenna B. The NLK-GA and NAU-GA data were received on antenna A, whereas the NSS-GA and NAA-GA data were received on antenna B. During December 1992, NAA turned off/on 52 times at night, for 8 of which only amplitude data are available. Of the 52 off/on episodes, 38 occurred during the period 0000-0030 UT. In 41 of the 52 episodes, the amplitude and/or phase of the NSS-GA probe wave was detectably perturbed. These signal perturbations represented a temporary cooling of the *D* region electrons when the NAA transmitter turns off (Figure 2). In the light of the emphasis of this research on ionospheric heating, the leading edges of the amplitude and phase perturbations were measured and subsequently inverted before being tabulated. The leading edges were considered because NAA did not always turn back on immediately to full power (e.g., Figure 2, right side). Indeed, in four cases NAA simply turned off at 1000 UT for the rest of the night. Figure 3 is a scatter plot of the 41 observed pairs of amplitude and phase changes recorded in this manner. The amplitude perturbations (ΔA) ranged from −0.11 to +0.84 dB, while the phase changes ($\Delta\phi$) ranged from 0 to −5.3°. The thresholds of detectability of amplitude and phase changes were approximately 0.1 dB and 0.5°, respectively. In one well-defined case (Figure 2, right side), the amplitude and phase of NSS-GA are perturbed by +0.32 dB and −2.7°, respectively. These perturbations are superposed on slow background variations that in the case of phase are largely due to local oscillator drift.

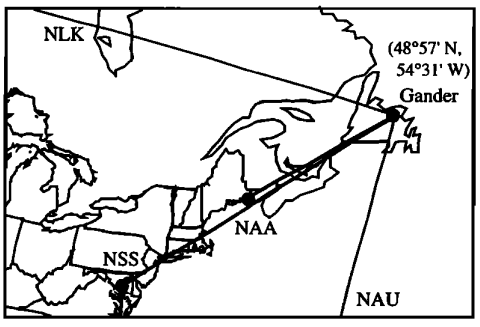

Figure 1. Map of North America and the Atlantic Ocean showing the great circle paths of subionospheric VLF probe waves observed at Gander, Newfoundland, during December 1992. This observational configuration was targeted to observe heating by the NAA transmitter using the NSS-Gander probe wave, whose 2063-km great circle path passes within 53 km of NAA.

In 6 of these 41 episodes, the NAU-GA probe wave amplitude was also perturbed (Table 2). In the case shown in the left half of Figure 2, the amplitude perturbation on NAU-GA due to NAA heating is +0.29 dB, and the associated amplitude and phase perturbations on NSS-GA are 0.84 dB and −1.5°, respectively. All but one of the six perturbations on NAU-GA were positive, and no phase perturbation was ever observed. In contrast, no detectable associated perturbations were observed on the NLK-GA signal. The observations of perturbations on the NAU-GA signal caused by NAA are surprising in the light of the > 770 km distance between NAA and the NAU-GA great circle path (Figure 1).

Since both the probe and heater wave signals are measured with the same apparatus, it is important to determine [*Inan*, 1990a] whether the observed cross-modulation between the two signals could have occurred within the receiver. The nonlinear cross-modulation response of the receiver at Gander was determined by locally injecting a 3-s on/2-s off 24.0-kHz signal into the terminals of either antenna and performing superposed epoch analysis of (typically) 60 min of data from VLF transmitter signals received concurrently [*Rodriguez*, 1994]. With a 24.0-kHz 140-mV m^{-1}-equivalent signal injected into the terminals of antenna B, the cross-modulation on NSS-GA was +0.02 dB

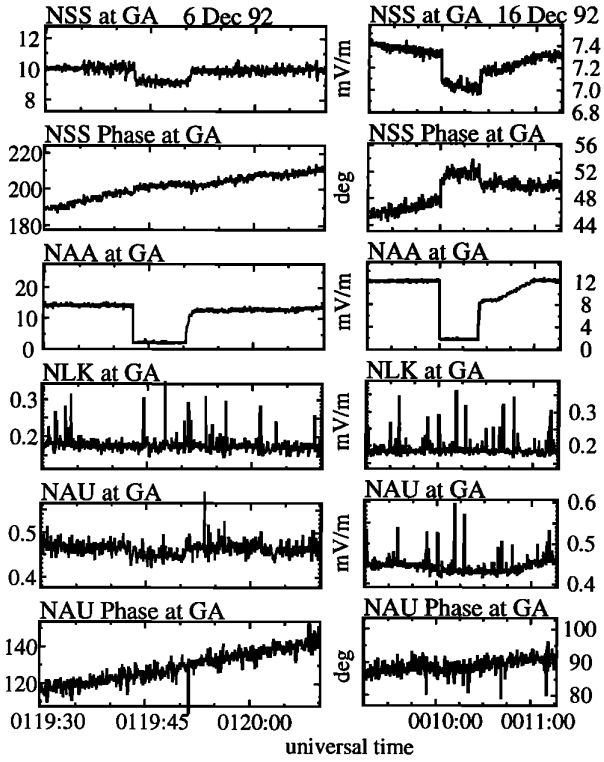

Figure 2. Heating by NAA observed at Gander (GA). (Left) NAA heating measured with the NSS-GA probe wave amplitude and phase and the NAU-GA amplitude on December 6, 1992. The NAA-GA field strength on antenna A (not shown) is 3.5 mV m^{-1}. NLK-GA amplitude and NAU phase are not affected. (Right) NAA heating measured with the NSS-GA probe wave amplitude and phase on December 16, 1992. NLK-GA amplitude and NAU-GA amplitude and phase are not affected. Note that the horizontal scales of the left and right panels are different. In both cases the linear vertical scale shows electric field in millivolts per meter or phase in degrees.

and +0.2°, while at 34-mV m^{-1}-equivalent there was no perturbation of NSS phase or amplitude. With a 24.0-kHz 82-mV m^{-1}-equivalent signal injected into the terminals of antenna A, the cross-modulation on NAU-GA was −0.1 dB and −1°; NLK was perturbed +1.6 dB due to its proximity in frequency to NAA. At 31-mV m^{-1}-equivalent there was no perturbation of NAU phase or amplitude. By comparison the field strength of NAA-GA received on antenna B at times of NAA off/on episodes during December 1992 ranged from 6.5 to 34 mV m^{-1}, while on antenna A it was always < 8.4 mV m^{-1}. That is, the received NAA-GA field strengths were much less than the injected 24.0-kHz equivalent field strengths required to cause measureable cross-modulation within the receiver. We therefore conclude that the observed cross-modulation between NAA and the NSS-GA and NAU-GA probe waves (Figure 2) occurred in the ionosphere, consistent with NAA heating the *D* region.

The NLK Transmitter as an Ionospheric Heater

In the second VLF heater-probe wave configuration considered here (Figure 4), the 23.4-kHz NPM signal propagating from Lualualei, Oahu, to Saskatoon, Saskatchewan (NPM-SA), was used to detect ionospheric heating by the NLK transmitter operating at 24.8 kHz with a nominal total radiated power of 850 kW. Between October 29 and November 23, 1987, 18 days of usable VLF probe wave amplitude data were recorded at Saskatoon from a geomagnetic north-south loop antenna, including 44 NLK off/on episodes, in four of which the NPM-SA probe wave was perturbed (Table 3). In the clearest of the four detectable cases, which occurred on October 29, 1987 (Figure 5), the response of the NPM-SA amplitude to heating (NLK on) is −1.0 dB. In all four cases, the other probe waves observed at Saskatoon (Figure 4) are not affected.

During the period considered here, intermittent interference was observed in the 23.40 ± 0.15 kHz band at Saskatoon that probably emanated from the 23.4-kHz transmitter in Rhauderfehn, Germany. The Rhauderfehn signal is readily observable in the Canadian Arctic [*Lauber and Bertrand*, 1993]. The interference from the Rhauderfehn signal may have affected our ability to detect NLK heating using the NPM-SA probe wave.

The NSS Transmitter as an Ionospheric Heater

In the third VLF heater-probe wave configuration considered here (Figure 6), the NAA signal observed at Huntsville, Alabama (NAA-HU), was used to detect ionospheric heating by the NSS transmitter operating at 21.4 kHz with a nominal total radiated power of 265 kW. During February 1990 there were 29 NSS off/on episodes, in five of which the

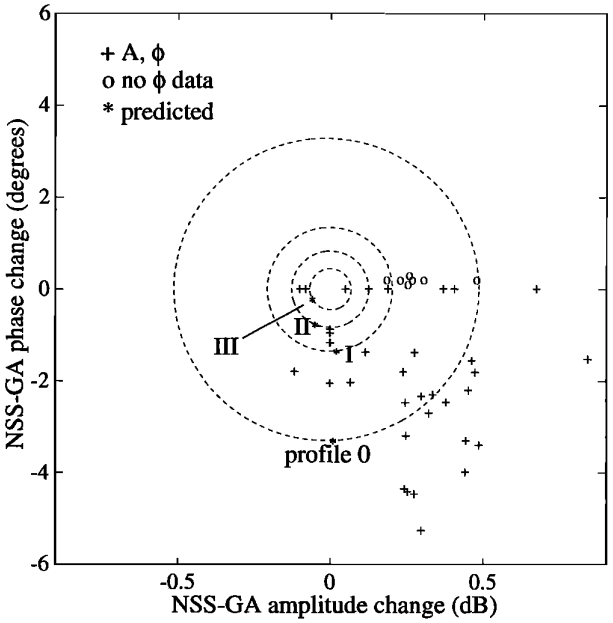

Figure 3. NSS amplitude and phase perturbations observed at Gander during NAA off/on episodes in December 1992, and perturbations predicted using the heating and waveguide propagation models. Open circles indicate that no phase (ϕ) data were available; these points have been plotted slightly off the $\Delta\phi = 0$ axis for clarity. The thresholds of detectability were approximately ±0.1 dB and ±0.5°. Asterisks labeled 0, I, II, and III indicate the predictions for the corresponding electron density profiles. Loci (dashed lines) are generated by varying the relative phase of the unperturbed and scattered signals from 0 to 2π.

Table 2. NAA Heating Detected by the NAU-GA Probe Wave

Date, 1992	Time, UT	Observed ΔA, dB	Observed $\Delta\phi$, °
Dec. 6	0119	+0.29	0
Dec. 6	0407	+0.07	0
Dec. 7	0914	+0.23	0
Dec. 7	1000	+0.22	0
Dec. 17	0010	+0.20	0
Dec. 28	0010	−0.09	0
	N_e Profile	Calculated ΔA, dB	Calculated $\Delta\phi$, °
	0	0.000	−0.093
	I	0.029	−0.015
	II	0.009	−0.004
	III	0.000	−0.004

Table 3. Observations of VLF Heating at Saskatoon (SA) and Huntsville (HU)

Date, 1987	Time, UT	NPM-SA ΔA, dB
Oct. 29	0704	−1.0
Nov. 7	0856	−1.6
Nov. 7	1242	+0.6
Nov. 21	0548	−0.3
Date, 1990	Time, UT	NAA-HU ΔA, dB
Feb. 12	2358	+0.2
Feb. 14	0808	+0.5
Feb. 16	2358	+0.2
Feb. 26	2358	+0.3
Feb. 27	0000	+0.5

NAA-HU amplitude increased in response to NSS heating (Table 3). Four of the five cases occurred within 2 min of 0000 UT, while only eight of the 29 off/on episodes occurred at this time. The other probe waves, received off the single loop antenna at Huntsville (its plane oriented geomagnetic north-south), were not affected in any of the episodes. In the clearest case, which occurred on February 14, 1990 (Figure 7), the response of the NAA-HU amplitude to heating (NSS on) is +0.5 dB. The small decrease in the NAU-HU amplitude occurring 10 s after NSS turned off may have been due to a lightning-induced disturbance along the NAU-HU great circle path. The 48.5-kHz off/on episodes occurred at the transmitter. In the case of February 12, 1990, the perturbation is much weaker (Figure 7).

Dependence on Geomagnetic Conditions

The ability of VLF transmitters to heat the *D* region and the sensitivity of subionospheric VLF probe waves to this heating depend on the ambient electron density and temperature of the *D* region. Geomagnetic activity is one possible cause of night-to-night variability in the *D* region

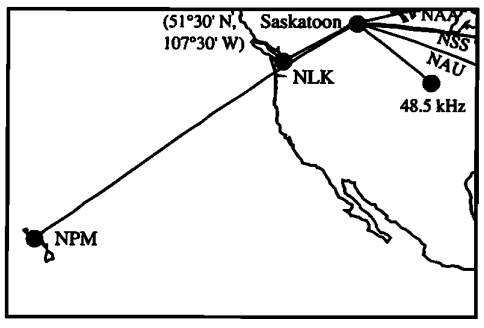

Figure 4. Map of North America and the Pacific Ocean showing the great circle paths of subionospheric VLF probe waves observed at Saskatoon, Saskatchewan, during October-November 1987. Heating by NLK was discovered serendipitously using this configuration. The only probe wave affected by NLK heating was the NPM-Saskatoon probe wave, whose 5469-km great circle path passed within 79 km of NLK.

electron density since it is associated with increased levels of energetic (> 20 keV) electrons precipitated from the Earth's radiation belts into the nighttime *D* region, resulting in secondary ionization and hence increased electron density, which in turn affects subionospheric VLF propagation [*Potemra and Rosenberg*, 1973; *Voss and Smith*, 1980].

One measure of geomagnetic activity is the planetary 3-hour *Kp* index. In the case of NAA heating measured by the NSS-GA probe wave during December 1992, the *Kp* indices for the periods preceding and concurrent with the 52 NAA off/on episodes ranged from 0 to 6+, with no apparent relation between size of perturbation and *Kp*. For the six NAA heating events observed on NAU-GA during December 1992, the preceding and concurrent *Kp* indices ranged from 0 to 5−. In the case of the four observed NLK heating events observed on NPM-SA during October and November 1987, *Kp* indices during the preceding and concurrent 3-hour period ranged from 1− to 4. As regards the five NSS heating events observed on NAA-HU, February 1990 was a fairly disturbed month according to the *Kp* indices, with even the quietest day (February 12) being "not really quiet." The *Kp* indices for the 3-hour periods preceding and including the NSS heating event of February 12, 1990, were 0+; for the other four events, the *Kp* indices ranged from 4 to 6+. In general, therefore, there is no evidence in the data analyzed here that either the VLF heating process itself or its detection by subionospheric VLF probe waves at mid-latitudes is affected by the level of geomagnetic activity as measured by the planetary 3-hour *Kp* indices. This finding is consistent with the conclusions of *Inan et al.* [1992] based on an analysis of a different data set.

In this connection it is interesting to consider whether some of the observed perturbations attributed to VLF heating could instead be due to transmitter-induced precipitation of energetic electrons from the Earth's radiation belts, whose population depends on geomagnetic activity. Precipitation was ruled out as a possible cause of the events observed in the experiment of *Inan* [1990a] because there was no delay between the observed cross-modulation on NAA-Palmer and the on/off pattern of the NAU heating transmitter, an observation strengthened by the presence of immediate, sharp event onsets and cessations. In the data sets analyzed in this paper, some of the observed events appear not to have such sharp onsets and cessations due to high lev-

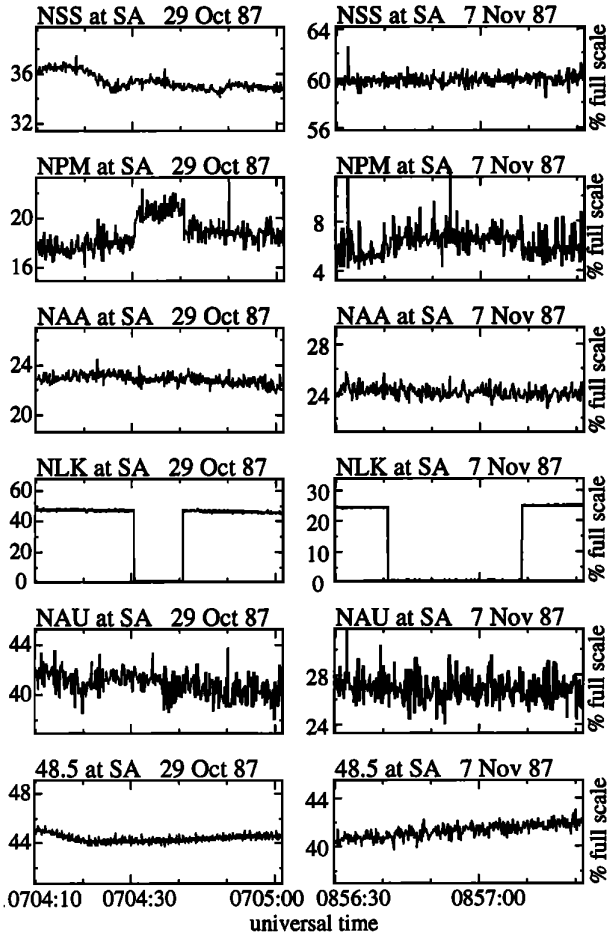

Figure 5. Heating by NLK observed at Saskatoon (SA). (Left) Fifty seconds of amplitude data showing NLK heating as detected using the NPM-SA probe wave on October 29, 1987. The response to NLK turning on (heating) at 0704:40 UT is –1.0 dB. (Right) Fifty seconds of amplitude data showing NLK heating as detected using the NPM-SA probe wave on November 7, 1987. The response to NLK turning on (heating) at 0704:40 UT is –1.6 dB. In both cases, the NSS, NAA, NAU, and 48.5-kHz signal amplitudes are not affected by the NLK heating.

els of atmospheric noise, which necessitate substantial block averaging of the signal to reveal the perturbation. However, the lack of such sharp signatures does not necessarily allow for precipitation to be a possible cause. Satellite-based in situ observations of energetic electrons precipitated by the keying of NAA and NSS reveal a ~1–2 s delay between transmitter turn-on and the electron precipitation [*Imhof et al.*, 1983a,b], consistent with theoretical expectations [*Inan et al.*, 1985]. No such delay is observed in the events studied here, and none of the observed perturbations lasts beyond the end of the causative heater off/on episode. In fact, some NAA off/on episodes and their associated NSS perturbations last less than 1 s. The timing aspects of the present data set and that of *Imhof et al.* [1983a,b] enable us to conclude that there is no evidence of transmitter-induced electron precipitation in the data studied here.

Electron Temperature Enhancements in the Nighttime *D* Region Due to Heating by VLF Transmitters

The nature of the evidence presented here of cross-modulation between VLF transmitter signals in the Earth-ionosphere waveguide suggests that the cross-modulation is due to heating of the *D* region over one of the transmitters resulting in a change in the electron collision frequency (and thus the electrical conductivity), which in turn affects the propagation of the other signal [*Inan*, 1990a]. The first step in the interpretation of the data using the predictions of theoretical models is a quantitative description of the heated region using a model of heating of free electrons by a VLF wave in a weakly ionized plasma [*Inan et al.*, 1992; *Barr and Stubbe*, 1992]. The amount of heating by the VLF wave is determined from the steady state balance between the rate of energy gained by the electrons from the wave and lost to N_2 and O_2 through elastic collisions and inelastic collisions involving rotational and vibrational excitation of the neutral molecules. The energy balance equation is $U = \sum_{i=1}^{3} [L_i(\mathrm{e},\mathrm{N}_2) + L_i(\mathrm{e},\mathrm{O}_2)]$ (J m^{-3} s^{-1}), where U is the sum of the powers dissipated in a unit volume by both magneto-ionic components and the cooling rates L_i are functions of electron and neutral temperatures T_e and T_n, with $i = 1, 2, 3$ representing elastic collisions, rotational excitation, and vibrational excitation [*Schunk and Nagy*, 1978; *Barr and Stubbe*, 1992]. Following *Barr and Stubbe* [1992], the refractive indices are determined assuming a momentum-transfer collision frequency proportional to electron kinetic energy and a Maxwellian electron distribution [*Sen and Wyller*, 1960; *Hara*, 1963].

In this three-dimensional model [*Inan et al.*, 1992], which assumes planar geometry, the time-averaged Poynting flux S is determined at the starting altitude from the transmitter's total radiated power and radiation pattern, assumed to be the toroidal pattern of an electrically short vertical dipole. The Poynting flux is calculated along straight lines originating at the transmitter and distributed regularly in elevation and azimuth angles. Refraction, reflection, and coupling between the ordinary and extraordinary components are neglected. At each altitude, $U = 2\omega\chi S/c$ is calculated for each magneto-ionic component, where ω is the

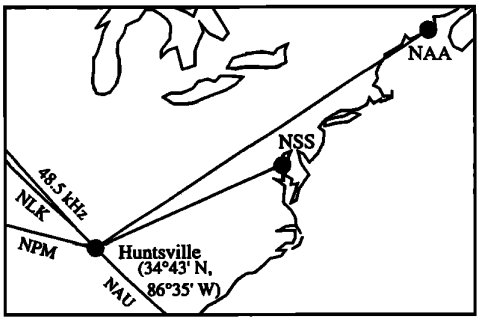

Figure 6. Map of a portion of North America showing the great circle paths of subionospheric VLF probe waves observed at Huntsville, Alabama, during February 1990. Heating by NSS was discovered serendipitously using this configuration. The only probe wave affected by NSS heating was the NAA-Huntsville probe wave, whose 1977-km great circle path passed within 160 km of NSS.

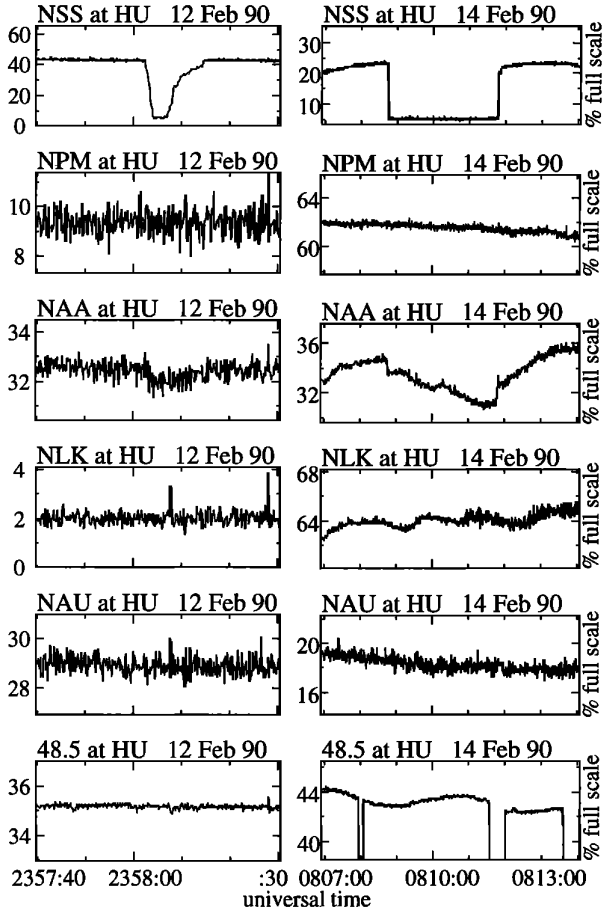

Figure 7. Heating by NSS observed at Huntsville (HU). (Left) Fifty seconds of amplitude data showing NSS heating as detected by the NAA-HU probe wave on February 12, 1990. The response to NSS turning gradually back on (heating) is +0.2 dB. (Right) Seven minutes of amplitude data showing NSS heating as detected by the NAA-HU probe wave on February 14, 1990. The response to NSS turning on (heating) at 0811:45 UT is +0.5 dB. The slower variations are typical of NAA during this period. In both cases, the NPM, NLK, NAU, and 48.5-kHz amplitudes are not affected by the NSS heating.

angular wave frequency, χ is the negative imaginary part of the refractive index, and c is the speed of light in free space. The electron-neutral collision frequency used to calculate χ at each altitude is the sum of the ambient collision frequency at that altitude and the change in collision frequency due to heating at the previous altitude. The energy balance equation is solved iteratively at each altitude for the heated electron temperature, and the increased collision frequency ν is given by $\nu = (T_e/T_n)\nu_o$, where ν_o is the ambient average momentum-transfer collision frequency.

The ambient collision frequency profile [*Wait and Spies*, 1964] and the four nighttime electron density profiles [*Barr and Stubbe*, 1992; *Inan et al.*, 1992] used in this paper are shown in Figure 8. The ambient temperature profile used is from the U.S. Standard Atmosphere (1976), as are the neutral density profiles below 86 km. The neutral density profiles above 86 km are from the mass spectrometer/incoherent scatter (MSIS-86) thermospheric model [*Hedin*, 1987].

The heated region is represented as the vertical collision frequency profile through the point (x_m, y_m, h_m) of maximum heating (defined as maximum $\Delta\nu/\nu_o$), scaled by the transverse structure of the heated region at the altitude of maximum heating h_m [*Inan et al.*, 1992]:

$$\Delta\nu(x,y,h) = \Delta\nu(x_m,y_m,h)\left[\frac{\Delta\nu(x,y,h_m)}{\Delta\nu(x_m,y_m,h_m)}\right]. \quad (1)$$

Shown on the left half of Figure 9 are profiles of the normalized collision frequency change $\Delta\nu(x_m,y_m,h)/\nu_o(h)$ due to heating by NSS, NLK, and NAA, predicted for electron density profiles 0, I, II, and III (Figure 8). On the right half are contour plots of $\Delta\nu(x,y,h_m)/\nu_o(h_m)$ over a 500 by 500 km area predicted for the case of profile 0.

Both the altitude and magnitude of maximum heating are higher for the more tenuous D regions used here. In the case of the most tenuous D region (profile 0), heating by NAA increases the electron temperature by as much as a factor of 3. In each case, there is a secondary peak in the heating in the altitude range where the extraordinary component is maximally absorbed and reflected, corresponding to the condition $\omega_{pe}^2 \simeq \omega_{ce}\omega$, where ω_{pe} and ω_{ce} are the electron plasma frequency and gyrofrequency, respectively, and ω is the wave frequency [*Ratcliffe*, 1959; *Rodriguez*, 1994]. Due to the toroidal radiation pattern of the transmitter, the heating is minimum (ideally zero) directly above the transmitter. At $h_m = 87.1$ km over NAA (profile 0) the radius at the outer half-maximum of $\Delta\nu(x,y,h_m)/\nu_o(h_m)$ is about ~ 150 km.

The heated regions are characterized by an asymmetry in the geomagnetic north-south direction [*Galejs*, 1972; *Inan et al.*, 1992], with maximum heating north (poleward) of the transmitter near a 45° elevation angle, corresponding to a direction of propagation nearly transverse to the Earth's magnetic field. Under this "quasi-transverse" condition of propagation, the ordinary magneto-ionic component is affected little by the Earth's magnetic field [*Ratcliffe*, 1959]. Consequently, it is maximally absorbed [*Galejs*, 1972; *Rodriguez*, 1994], resulting in the north-south asymmetry in the heated region.

The prediction here of $\max\{\Delta\nu(x_m,y_m,h)/\nu_o(h)\} = 2.17$ at 87.1 km altitude for the 1000-kW NAA transmitter and

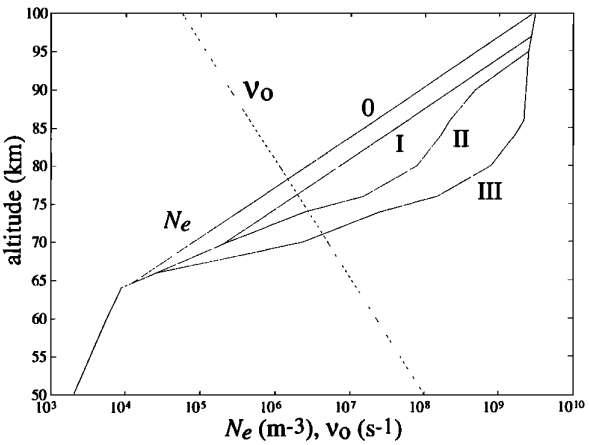

Figure 8. Electron density (N_e) and average electron-neutral collision frequency (ν_o) profiles used. Profile 0 is from *Barr and Stubbe* [1992]; profiles I, II, and III are from *Inan et al.* [1992]. The collision frequency profile is from *Wait and Spies* [1964].

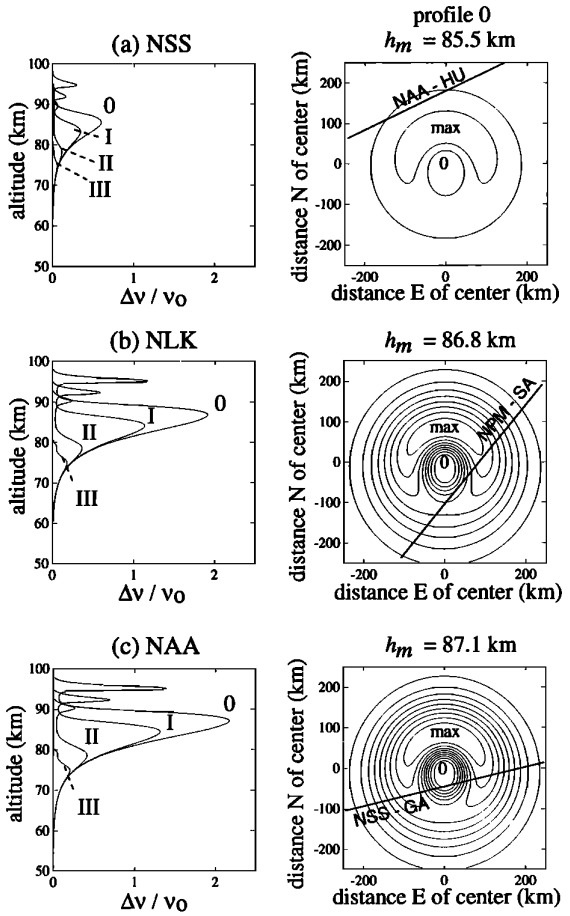

Figure 9. Vertical and transverse variation of the increase in *D* region electron collision frequency over NSS, NLK, and NAA. (Left) Calculated $\Delta\nu(x_m, y_m, h)/\nu_o(h)$ profiles and (right) contour plots of $\Delta\nu(x, y, h_m)/\nu_o(h_m)$ over (a) NSS, (b) NLK, and (c) NAA. The profiles are shown for electron density profiles 0 (most tenuous), I, II, and III (most dense), and the transverse variations are shown for profile 0. In each case the great circle path of the probe wave that is closest to the heating transmitter is superposed on the contour plot. Geomagnetic north is toward the top of the page.

profile 0 (Figure 9c) is much larger than the prediction by *Barr and Stubbe* [1992] of $\max\{\Delta\nu(x_m, y_m, h)/\nu_o(h)\} = 0.72$ for the same transmitter and electron density profile. The same prediction using our model but with the collision frequency profile of *Barr and Stubbe* [1992] is $\max\{\Delta\nu(x_m, y_m, h)/\nu_o(h)\} = 1.84$ at 87.5 km [*Rodriguez*, 1994]. The remaining discrepancy is due in large part to the fact that *Barr and Stubbe* [1992] treated only vertical incidence of the NAA transmitter signal on the *D* region, whereas maximum heating is expected for $\sim 45°$ incidence in the poleward direction from the transmitter, as discussed above.

Effect of VLF Heating of the Nighttime *D* Region on Subionospheric VLF Probe Waves

A multiple-mode three-dimensional model of VLF propagation in the Earth-ionosphere waveguide [*Poulsen et al.*, 1993a,b] is used to calculate the vertical electric field of the probe wave at the receiver in the absence and in the presence of heating, the difference between which gives the resulting amplitude and phase changes. The ambient *D* region electron density profile is assumed constant along the great circle path of the probe wave, but the magnetic dip angle and ground conductivity are allowed to vary, resulting in mode coupling along the great circle path. The standard magneto-ionic theory [*Ratcliffe*, 1959], which assumes an effective electron-neutral collision frequency (ν_{eff}) that is independent of electron energy, is used to calculate the refractive indices S_n of the waveguide modes. In order that the predictions of maximum heating using the theory of *Sen and Wyller* [1960] are consistent with the waveguide propagation model, we use the relation $\nu_{\text{eff}} = \nu$, where ν is the average momentum-transfer collision frequency in a Maxwellian velocity distribution [*Sen and Wyller*, 1960]. This relation is valid for propagation quasi-transverse to the Earth's magnetic field assuming $\nu \gg \omega$ [*Deeks*, 1966], which condition is adequate below 90 km and strictly true below 80 km in our model ionosphere (Figure 8).

Although the complex refractive index S_n of mode n depends nonlinearly on ν, numerical analysis [*Rodriguez*, 1994] shows that even for a factor of 3 increase in collision frequency (Figure 9c), $\Delta S_n \propto \Delta\nu$ for all but the highest-order modes, which contribute insignificantly to the received signals. Such linearity, which has been demonstrated for an order of magnitude increase in the collision frequency [*Barr et al.*, 1985], is due to the fact that since $\nu \ll \omega_{ce}$ above 75 km in the midlatitude ionospheres considered here, the refractive indices for all but "quasi-transverse" propagation are dominated by the Earth's magnetic field rather than the electron-neutral collision frequency [*Barr et al.*, 1985; *Rodriguez*, 1994]. Consequently, the refractive index for each mode is calculated at each point in the heated region as

$$S_n(x, y) = S_n^o + [S_n(x_m, y_m) - S_n^o] \frac{\Delta\nu(x, y, h_m)}{\Delta\nu(x_m, y_m, h_m)} \quad (2)$$

where S_n^o and $S_n(x_m, y_m)$ are the refractive indices of mode n for the ambient and heated collision frequency profiles, respectively.

The NSS-GA signal perturbations due to NAA heating predicted for electron density profiles 0, I, II, and III (Figure 8) are listed in Table 4 and are plotted in Figure 3 along with the observed amplitude and phase perturbations. The largest scattered fields are predicted for heating by NAA of the most tenuous *D* region (profile 0). The predictions for profiles I and III are each consistent with a few of the observed perturbations. However, the model fails to predict amplitude and phase change pairs consistent with the largest observed signal perturbations ($\Delta A > 0.25$ dB and $\Delta\phi < -2.0°$).

To better evaluate the effect of a possible error in the predicted scattered signal amplitude or phase on the amplitude

Table 4. Calculated NSS-GA Perturbations Due to NAA Heating

N_e Profile	ΔA, dB	$\Delta\phi$, °	max$\lvert\Delta A\rvert$, dB	max$\lvert\Delta\phi\rvert$, °
0	+0.01	−3.29	0.51	3.29
I	+0.02	−1.34	0.21	1.35
II	−0.05	−0.77	0.13	0.83
III	−0.06	−0.21	0.07	0.45

and phase perturbations, the loci of all possible phase and amplitude perturbation pairs are plotted in Figure 3 for the calculated magnitudes of the scattered fields. The amplitude perturbations are given in terms of the magnitude of the ratio

$$\frac{E_o + E_s}{E_o} = 1 + \left|\frac{E_s}{E_o}\right| \exp(i\phi_r) \quad (3)$$

expressed in dB, where E_o and E_s are the unperturbed and scattered vertical electric field phasors, respectively. The phase perturbations are given by the phase of this complex ratio. The loci are generated by varying ϕ_r, the phase of the scattered field relative to the unperturbed field, from 0 to 2π. The maximum possible amplitude and phase changes calculated in this manner for a given scattered field amplitude are also listed in Table 4. The locus of the scattered field E_s predicted for profile 0 passes through a group of several observed amplitude and phase perturbation pairs, including the December 16, 1992, event shown in Figure 2. It can be seen from Figure 3, for example, that if the difference between the phases predicted for profile 0 were $\sim 45°$ smaller, then the predicted amplitude and phase perturbations would be in good agreement with the observations. The range of predicted scattered field amplitudes is thus consistent with the observations to within a factor of 2, and ϕ_r is likely to be the primary source of the discrepancy. A 45° phase error corresponds to one-eighth of a wavelength, which at 21.4 kHz is 1.7 km, or less than 0.1% of the great circle path length between NSS and Gander. In general, given the uncertainties involved in modeling the *D* region at all points between NSS and Gander (a distance of 2063 km) with a single electron density profile, an error of such a magnitude ($\sim$ 2 km) in the optical path length of the unperturbed (E_o) or scattered (E_s) fields is not unexpected.

In the case of NLK heating detected with the NPM-SA probe wave the calculated amplitude changes (Table 5) are much smaller than, though mostly of the same polarity as, the observed values (Table 3). Even the maximum possible amplitude changes possible for the calculated scattered electric field amplitudes are smaller than the observed amplitude change magnitudes. However, it is possible that the interference from the Rhauderfehn transmitter obscured weaker perturbations that might have been closer to the predictions.

In the case of NSS heating detected with the NAA-HU probe wave, the amplitude changes predicted for electron density profiles 0 and I (Table 6) are consistent with the magnitude of some of the observed perturbations, but opposite in polarity to all of the observed values (Table 3). Note that for profiles 0, I, and II the magnitudes of the predicted amplitude changes are essentially the same as the maximum changes possible for the calculated scattered electric field amplitudes.

Table 5. Calculated NPM-SA Perturbations Due to NLK Heating

N_e Profile	ΔA, dB	$\Delta\phi$, °	max$\lvert\Delta A\rvert$, dB	max$\lvert\Delta\phi\rvert$, °
0	−0.08	−0.58	0.12	0.78
I	−0.07	−1.27	0.21	1.34
II	−0.01	−0.28	0.04	0.29
III	−0.01	−0.26	0.04	0.27

Table 6. Calculated NAA-HU Perturbations Due to NSS Heating

N_e Profile	ΔA, dB	$\Delta\phi$, °	max$\lvert\Delta A\rvert$, dB	max$\lvert\Delta\phi\rvert$, °
0	−0.24	−0.68	0.26	1.71
I	−0.24	−0.19	0.24	1.55
II	−0.11	−0.20	0.11	0.72
III	−0.01	−0.11	0.02	0.12

The fact that, in general, larger perturbations are observed on the NSS-GA, NPM-SA, and NAA-HU probe waves than can be explained by the predicted magnitudes of the fields scattered from the heated regions may be due in part to the fact that we neglect reflection effects in the heating model. *Galejs* [1972] showed that 20-25% larger vertical electric fields at $h = 85$ km are predicted when reflection is included. In the case of NLK heating, the larger discrepancies may also stem from the assumption of a single ambient *D* region electron density profile along the 5469-km NPM-SA probe wave great circle path. This long path covers a greater range of geomagnetic latitudes than the other two paths, being oriented nearly north-south geomagnetic; therefore latitudinal variations in electron density profile, possibly related to geomagnetic activity [*Potemra and Rosenberg*, 1973; *Voss and Smith*, 1980], may affect the NPM-SA path more than the NAA-HU or NSS-GA paths.

Due to the great distance of NAA from the NAU-GA great circle path ($\geq$ 770 km), scattering of the NAU signal from the center of the heated region (Figure 9c) toward Gander should be negligible since the disturbance satisfies the WKB approximation [*Poulsen et al.*, 1993b]. In order to model the effect of NAA on NAU-GA, therefore, we consider heating by the direct (half-hop) rays from NAA impinging on the ionosphere directly above the point on the NAU-GA great circle path closest to NAA (770 km in the direction 124° east of geomagnetic north from NAA), using spherical geometry. A two-dimensional waveguide calculation is then performed in which the heated region is modeled as a 100-km-long slab centered at this point. The maximum collision frequency changes calculated for the four electron density profiles, and the altitudes at which they are predicted to occur, are (0) 4.4% at 82 km, (I) 2.4% at 80 km, (II) 1.0% at 76 km, and (III) 0.5% at 73 km. Note that these increases at a distance of 770 km from the heating transmitter are very small compared to the maximum collision frequency changes predicted to occur near the transmitter (Figure 9c).

Predictions of the perturbation on the NAU-GA probe wave due to the predicted collision frequency changes are listed in Table 2. Except for the result predicted for profile I, they are all more than 1 order of magnitude smaller than the observations (Table 2). The smallest perturbation observed (0.07 dB) is still a factor of 2.4 larger than the 0.029 dB perturbation predicted for profile I. This relatively large perturbation on the NAU-GA probe wave is predicted to occur because, under profile I, Gander is located in a $\sim$ 10-dB relative minimum of the spatial pattern of the NAU-GA vertical electric field that makes it more sensitive to the heating by NAA. The NAU field strengths from Gander at the times of heating signatures are relatively low but do not strongly indicate the presence of a 10-dB null. Nevertheless, in the absence of knowledge of the actual state of the nighttime *D* region, the presence of a deep null in the

NAU probe wave vertical electric field at Gander appears to be a reasonable qualitative explanation for the observations of ionospheric cross-modulation between NAA-GA and NAU-GA during December 1992.

Summary and Conclusions

Calculations of scattering of subionospheric VLF probe waves by patches of increased D region collision frequency are in reasonable agreement with observed cross-modulation between subionospheric VLF waves, establishing that the effect is due to heating in the nighttime D region by VLF transmitters. Predictions of NAA heating were calculated for four nighttime D region electron density profiles varying over 2 orders of magnitude. The predicted radius at half-maximum of the heated patches is $\sim$ 150 km, and the electron temperature is increased in the most tenuous D region by a factor of 3. Predictions of NSS field amplitudes scattered from the heated region over NAA toward Gander are in general consistent with repeated observations of NSS-GA amplitude and phase perturbations during December 1992. Heating by NAA has also been observed on the NAU-GA probe wave, whose great circle path is 770 km from NAA at its closest approach. This unexpected observation is explained qualitatively by a null in the NAU-GA probe wave spatial pattern near Gander making it sensitive to weak heating by NAA along the NAU-GA great circle path under a relatively tenuous nighttime D region. Heating by NSS and NPM has also been observed, using the NAA-HU and NPM-SA probe waves, respectively. Predictions are in rough agreement with the limited number of observations in these cases. The observations and results of the theoretical models indicate that powerful VLF transmitters, typically operating continuously, regularly heat the nighttime D region overhead. One manifestation of such heating may be large-scale depletions in the D region electron density over VLF transmitters [*Rodriguez and Inan*, 1994]; other resulting effects remain to be investigated.

Acknowledgments. We thank our STAR Laboratory colleagues for their comments and assistance, in particular S. C. Reising, W. J. Trabucco, and D. S. Shafer with the experiments; C. M. Bradford with data analysis; and S. J. Lev-Tov and S. A. Cummer with the waveguide model. We are grateful to the 770 Communications Research Squadron in Gander, in particular B. Corbin, S. North, and T. Moss, for operating the Stanford system, and to D. McEwen and G. Fishman for their support of the operation of the Stanford systems at Saskatoon and Huntsville, respectively. This research was supported by ONR grant N00014-92-J-1579 to Stanford University. J. V. Rodriguez was supported during this work by a NASA Graduate Student Researchers Program fellowship.

The Editor thanks R. Barr and another referee for their assistance in evaluating this paper.

References

Barr, R., and P. Stubbe, VLF heating of the lower ionosphere: Variation with magnetic latitude and electron density profile, *Geophys. Res. Lett., 19*, 1747–1750, 1992.

Barr, R., M. T. Rietveld, P. Stubbe, and H. Kopka, The diffraction of VLF radio waves by a patch of ionosphere illuminated by a powerful HF transmitter, *J. Geophys. Res., 90*, 2861–2875, 1985.

Burgess, W. C., and U. S. Inan, The role of ducted whistlers in the precipitation loss and equilibrium flux of radiation belt electrons, *J. Geophys. Res., 98*, 15,643–15,665, 1993.

Deeks, D. G., Generalised full wave theory for energy-dependent collision frequencies, *J. Atmos. Terr. Phys., 28*, 839–846, 1966.

Galejs, J., Ionospheric interaction of VLF radio waves, *J. Atmos. Terr. Phys., 34*, 421–436, 1972.

Hara, E. H., Approximations to the semiconductor integrals $C_p(x)$ and $D_p(x)$ for use with the generalized Appleton-Hartree magnetoionic formulas, *J. Geophys. Res., 68*, 4388–4389, 1963.

Hedin, A. E., MSIS-86 thermospheric model, *J. Geophys. Res., 92*, 4649–4662, 1987.

Imhof, W. L., J. B. Reagan, H. D. Voss, E. E. Gaines, D. W. Datlowe, J. Mobilia, R. A. Helliwell, U. S. Inan, J. Katsufrakis, and R. G. Joiner, Direct observation of radiation belt electrons precipitated by the controlled injection of VLF signals from a ground-based transmitter, *Geophys. Res. Lett., 10*, 361–364, 1983a.

Imhof, W. L., J. B. Reagan, H. D. Voss, E. E. Gaines, D. W. Datlowe, J. Mobilia, R. A. Helliwell, U. S. Inan, J. Katsufrakis, and R. G. Joiner, The modulated precipitation of radiation belt electrons by controlled signals from VLF transmitters, *Geophys. Res. Lett., 10*, 615–618, 1983b.

Inan, U. S., VLF heating of the lower ionosphere, *Geophys. Res. Lett., 17*, 729–732, 1990a.

Inan, U. S., Modification of the lower ionosphere in lightning-induced electron precipitation events and through VLF heating, in Ionospheric Modification and Its Potential to Enhance or Degrade the Performance of Military Systems, *AGARD Conf. Proc., 485*, 29-1–29-12, 1990b.

Inan, U. S., H. C. Chang, R. A. Helliwell, W. L. Imhof, J. B. Reagan, and M. Walt, Precipitation of radiation belt electrons by man-made waves: A comparison between theory and measurement, *J. Geophys. Res., 90*, 359–369, 1985.

Inan, U. S., F. A. Knifsend, and J. Oh, Subionospheric VLF "imaging" of lightning-induced electron precipitation from the magnetosphere, *J. Geophys. Res., 95*, 17,217–17,231, 1990.

Inan, U. S., J. V. Rodriguez, S. Lev-Tov, and J. Oh, Ionospheric modification with a VLF transmitter, *Geophys. Res. Lett, 19*, 2071–2074, 1992.

Lauber, W. R., and J. M. Bertrand, VLF propagation measurements in the Canadian Arctic, in ELF/VLF/LF Radio Propagation and Systems Aspects, *AGARD Conf. Proc., 529*, 5-1–5-12, 1993.

Potemra, T. A., and T. J. Rosenberg, VLF propagation disturbances and electron precipitation at mid-latitudes, *J. Geophys. Res., 78*, 1572–1580, 1973.

Poulsen, W. L., U. S. Inan, and T. F. Bell, A multiple-mode three-dimensional model of VLF propagation in the Earth-ionosphere waveguide in the presence of localized D region disturbances, *J. Geophys. Res., 98*, 1705–1717, 1993a.

Poulsen, W. L., T. F. Bell, and U. S. Inan, The scattering of VLF waves by localized ionospheric disturbances produced by lightning-induced electron precipitation, *J. Geophys. Res., 98*, 15,553–15,559, 1993b.

Ratcliffe, J. A., *The Magneto-Ionic Theory and Its Applications to the Ionosphere*, 206 pp., Cambridge University Press, Cambridge, 1959.

Rodriguez, J. V., Modification of the Earth's ionosphere by very-low-frequency transmitters, Ph.D. dissertation, Stanford Univ., Stanford, Calif., 1994.

Rodriguez, J. V., and U. S. Inan, Electron density changes in the nighttime D region due to heating by very-low-frequency transmitters, *Geophys. Res. Lett., 21*, 93–96, 1994.

Schunk, R. W., and A. F. Nagy, Electron temperatures in the F region of the ionosphere: Theory and observations, *Rev. Geophys. Space Phys., 16*, 355–399, 1978.

Sen, H. K., and A. A. Wyller, On the generalization of the Appleton-Hartree magnetoionic formulas, *J. Geophys. Res., 65*, 3931–3950, 1960.

Voss, H. D., and L. G. Smith, Global zones of energetic particle precipitation, *J. Atmos. Terr. Phys., 42*, 227–239, 1980.

Wait, J. R., and K. P. Spies, Characteristics of the Earth-ionosphere waveguide for VLF radio waves, *NBS Tech. Note U.S., 300*, Dec. 30, 1964.

T. F. Bell and U. S. Inan, Space, Telecommunications and Radioscience Laboratory, Department of Electrical Engineering, Stanford University, Stanford, CA 94305-4055. (e-mail: Internet.bell@nova.stanford.edu; inan@nova.stanford.edu)

J. V. Rodriguez, Phillips Laboratory, Geophysics Directorate, PL/GPIA, Hanscom AFB, MA 01731. (e-mail: Internet.rodriguezr@plh.af.mil)

(Received March 21, 1994; revised July 15, 1994; accepted July 26, 1994.)